The surface residual stress of monocrystalline silicon in ultrasonic vibration assisted diamond wire sawing

YAN WANG (yanwang909909@163.com)
University of Shanghai for Science & Technology https://orcid.org/0000-0001-5808-1622
Bocheng Zhao
Jixing Li
Zhaofeng Qian
Shengju Huang
Jinhuan Su
Jing Zhou

Research Article

Keywords: Diamond wire sawing, Ultrasonic vibration assisted, Monocrystalline silicon, Residual stress, Blind hole drilling method

Posted Date: March 9th, 2022

DOI: https://doi.org/10.21203/rs.3.rs-1413561/v1

The surface residual stress of monocrystalline silicon in ultrasonic vibration assisted diamond wire sawing

Yan Wang [a, *], Bocheng Zhao [a], Jixing Li [a], Zhaofeng Qian [a], Shengju Huang [a], Jinhuan Su [a], Jing Zhou[a]

[a] School of Mechanical Engineering, University of Shanghai for Science and Technology, Shanghai, 200093, China

* Corresponding author, E-mail address: yanwang909909@163.com, Tel numbers: 021-55270938

Abstract: Monocrystalline silicon wafer is the most important raw material in chip manufacturing, wire sawing is the most common processing method of monocrystalline silicon wafer. The residual stress generated by cutting affects the subsequent polishing costs directly, as well as the fracture strength and mechanical integrity of the monocrystalline silicon wafer, thus affecting the service performance. In this paper, the generation mechanism of residual stress was analyzed based on diamond wire sawing technology. Then, based on D-P plastic constitutive model, the magnitude and distribution of residual stress of monocrystalline silicon chip under different process parameters were simulated by ABAQUS simulation software. Finally, the experiment of ultrasonic vibration assisted diamond wire sawing monocrystalline silicon and blind hole drilling method detection were conducted, the strain values before and after drilling in three directions were measured by strain gauge rosette, and the residual stress was calculated by combining with mathematical theory, and the experimental results verified the validity of the finite element model. The experimental results showed that residual compressive stress remains on the surface of silicon wafer in both conventional wire sawing and ultrasonic vibration assisted wire sawing. The residual compressive stress increases with the increase of the axial speed of wire saw, decreases with the increase of the wire saw feed speed, and fluctuates with the increase of the workpiece rotation speed. The residual compressive stress on the surface of the silicon wafer by ultrasonic vibration assisted wire sawing is larger than that by conventional wire sawing. The variation trend of simulation and experiment results is consistent, which provides theoretical support for the subsequent processing of monocrystalline silicon wafers.

Keywords: Diamond wire sawing; Ultrasonic vibration assisted; Monocrystalline silicon; Residual stress; Blind hole drilling method

1. Introduction

With the development of science and technology, semiconductor materials have attracted wide attention. Monocrystalline silicon is a kind of semiconductor material which is hard and brittle and difficult to process. It is widely used, especially in chip manufacturing. Wire sawing is the main processing method of slicing monocrystalline silicon wafers. It can be divided into free abrasive wire sawing, semi-fixed wire sawing and fixed abrasive wire sawing according to different types of wire saw. According to whether there is a multi-field auxiliary processing, the processing is divided into conventional wire sawing technology and ultrasonic vibration assisted wire sawing technology. Ultrasonic assisted machining has high frequency impact vibration and separation characteristics, which can effectively reduce the average cutting force and cutting temperature, thus improve the fatigue resistance, the surface quality and surface residual stress of the workpiece [1]. The residual stress is mainly caused by the cutting effect of wire saw, the cutting heat effect and the phase change

effect of workpiece, it will affect the fracture strength, mechanical integrity, magnetic properties and electrical properties of silicon crystal [2, 3]. However, a certain amount of residual compressive stress can improve the fatigue resistance of workpiece, so it is of great significance to further study the influence of diamond wire sawing process on the residual stress.

Residual stress measurement technology is the prerequisite for studying residual stress. After decades of theoretical research and engineering application, drilling method has formed a relatively mature technical system, which is the most widely method in residual stress measurement at present [4]. At present, scholars are studying methods for measuring residual stress of monocrystalline silicon wafers. Zheng et al. [5] proposed measuring the residual stress of full-size silicon wafers by near-infrared birefringence polariscopy method. Popovich et al. [6] used micro-Raman spectroscopy to detect residual stress in the damaged layer of MC-Si chip slicing. Babaeeian et al. [7] compared the method of hole-drilling by applying the rosette strain gauge with the digital image correlation (DIC) method to detect the residual stress on the composite plate. Mohr's circle method is used in the above comparison. Zhou et al. [8] comprehensively investigated the effects of cutting speed on surface roughness, subsurface damage, residual stress, and grinding force for a constant grain depth-of-cut. The results illustrate that the changes in residual stress relative to the grinding speed are less obvious when the material is removed in ductile-mode as opposed to in the brittle-duc-tile mixed mode. Jiao et al. [9] studied the nanoindentation of monocrystalline silicon at 1K using molecular dynamics simulation method, and studied the force-displacement curve and corresponding phase transition process in detail. They also found that the phase distribution during the reverse transformation was strongly influenced by the indenter radius and in-dentation depth due to the different stress fields. Echizenya et al. [10] established a function relationship between stress and etching depth, and the results showed that the residual compressive stress decreased with the increase of wafer depth. Wurzner et al. [11] used one single abrasive to scratch monocrystalline silicon and detected the residual stress through Raman spectroscopy. The results showed that the residual stress generated by scratching was compressive stress, however the residual stress is not quantified. Dai et al. [12] studied the ultra-precision machining of monocrystalline silicon by using 3d molecular dynamics (MD) simulation method. The advantages and disadvantages of structured and unstructured tools in machining diamond are discussed by comparing with those of unstructured tools. Yang et al. [13] etched the silicon wafer by diamond wire saw slicing with HF/HNO3 solution, and the comparative analysis results of the trend of residual stress before and after etching showed that the maximum residual shear stress and average residual shear stress in the silicon wafer decreased after etching. Kumar et al. [14] studied the maximum residual shear stress of the silicon wafer by diamond wire saw slicing at different growth rates, and detected the distribution of residual stress field inside the wafer through the near infrared transmission double-emission polarization method. The results showed that fast-growing wafer crystal had a large maximum residual shear stress. Erick et al. [15] studied the influence of different slicing parameters on monocrystalline silicon wafers, and measured the residual stress of the silicon wafers after cutting by Raman spectroscopy. The results showed that the residual stress on the surface of the monocrystalline silicon wafer by wire saw slicing is compressive stress, and the residual compressive stress increases with the increase of the axial speed of the wire saw. The residual stress decreases with the increase of feed speed. Yang et al. [16] investigated machining-induced surface damages such as surface fracture, phase transition, and residual stress, and revealed the surface damage mechanism for micro ball-end milling of mono-crystalline silicon. Pogue et al. [17] studied the influence of free abrasive

wire sawing and fixed abrasive wire sawing on the residual stress. The photoelastic method was used to detect the residual stress of the whole layer, and the micro-Raman spectroscopy was used to detect the residual stress on the silicon wafer surface. The results showed that the residual compressive stress on the surface of the silicon wafer is produced by the fixed abrasive wire sawing and the free abrasive wire sawing, and the residual compressive stress produced by the free abrasive wire saw is greater, but there is lower residual tensile stress under the damaged layer of the silicon wafer. Banerjee et al. [18] analyzed the debris generated after cutting silicon ingots with diamond abrasives coated wire saw by Raman spectroscopy. The results showed that one kind of granular chip is crystalline with residual compressive stress, and the other is amorphous with fibrous chip with residual tensile stress.

At present, scholars have also made some progress in the simulation of residual stress. Kiyota et al. [19] proposed a model to compute the mechanical stress and the geometry of the cracks formed by subsurface nanosecond-pulsed laser modification within monocrystalline silicon wafers, and confirmed the residual stress generation due to material transfer caused by volume reduction during melting and resolidification to be the dominant factor in creating subsurface mechanical stress and cracks. Zhang et al. [20] established a thermodynamic coupling cutting simulation model for two-dimensional orthogonal cutting of titanium alloy based on J-C constitutive through ABAQUS, and analyzed the distribution of residual stress under ultrasonic vibration cutting and conventional cutting. Chen et al. [21] studied the phase transformation and distribution of residual stress in ground silicon wafers by step-wire wet etching and confocal laser micro-Raman spectroscopy, and explained the grinding mechanism and the cause of induced residual stress in ground silicon. The results showed that the residual stress of the machined surface is tensile stress, which gradually transitions from tensile stress to compressive stress along the depth direction. With ultrasonic vibration assisted, the residual tensile stress on the workpiece surface is smaller and the maximum residual compressive stress is larger than that in conventional cutting. Liu et al. [22,23] considered the finite element method of silicon anisotropy and used it to analyze the deformation process, then extracted the surface characteristics of the deformed silicon wafer, and finally obtained the residual stress threshold at the bifurcation point by using the linearization technology according to the changing law of deformation characteristics. Xu et al. [24] established a two-dimensional orthogonal thermodynamic coupling model of Aluminum alloy by ABAQUS, and compared the residual stress of surface layer in conventional cutting, transverse ultrasonic vibration cutting with longitudinal ultrasonic vibration cutting. The results showed that the surface residual stress in above three different cutting methods are all compressive stress, and the residual tensile stress is transferred along the depth direction, and ultrasonic vibration cutting can significantly increase the surface residual compressive stress. The surface residual compressive stress decreases with both increase of cutting speed and cutting depth, while the residual surface compressive stress also increases with vibration amplitude or frequency. The above literature mainly studied the detection of residual stress on the surface of silicon wafer, but the residual stress of ultrasonic vibration assisted diamond wire sawing monocrystalline silicon wafer was not discussed and studied. After the ultrasonic vibration assisted is applied, the relative trajectory between the abrasives and the workpiece changes from continuous contact to intermittent contact. With the ultrasonic vibration assisted wire sawing, abrasives impact the workpiece constantly, the internal stress state of the workpiece changes accordingly.

Firstly, the principle of diamond wire sawing technology was analyzed in this paper, and a

simulation model of diamond wire sawing monocrystalline silicon was established by ABAQUS based on D-P constitutive, and the magnitude and distribution of residual stress under different process parameters were simulated. Finally, ultrasonic vibration assisted diamond wire sawing monocrystalline silicon experiment and blind hole drilling method experiment were carried out to detect the residual stress. Strains in three directions were measured with strain flower, and the variation trend of residual stress was analyzed with the theory of blind hole method measurement.

2. Principle of ultrasonic vibration assisted diamond wire sawing

Fig. 1 shows the schematic diagram of ultrasonic vibration assisted diamond wire sawing monocrystalline silicon. The whole system can be divided into wire saw feed mechanism and workpiece rotation mechanism, which is composed of a wire barrel, two tensioning wheels, two leading wheels, an auxiliary guide wheel, an ultrasonic guide wheel and a loading tray. During cutting process, the wire saw is subjected to constant tensioning force F_t from the cylinder. The diamond wire saw wound on the wire barrel is driven by the motor to move around the tensioning wheel, the leading wheel and the auxiliary wheel at reciprocating speed of v_s. At the same time, diamond wire saw moves downward with line speed v_w. The monocrystalline silicon workpiece is bonded to the loading tray, and the self-rotating motion with speed n_w is realized by a motor drive. The ultrasonic vibration is applied to the ultrasonic regulating wheel, with amplitude A and frequency f respectively. In order to enhance the lubrication effect and reduce sawing heat during wire sawing, a mixture of water and grinding fluid is used as coolant.

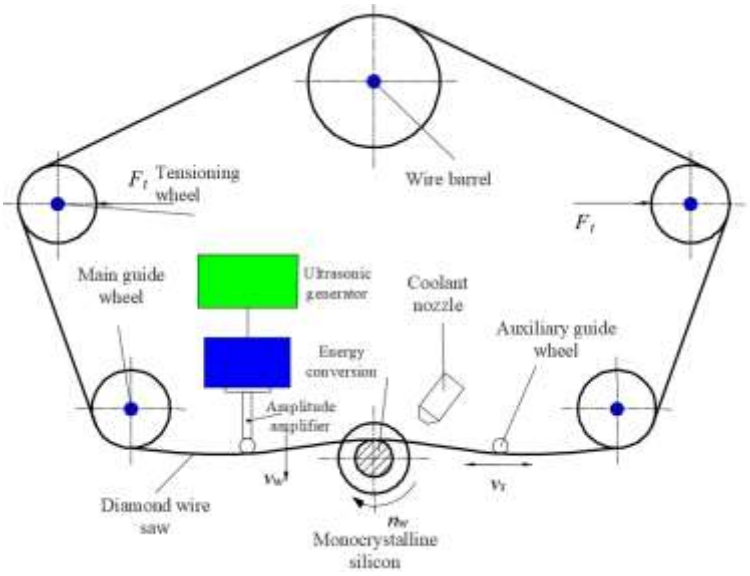

Fig. 1. Schematic diagram of ultrasonic vibration assisted diamond wire sawing monocrystalline silicon

2.1 Generation mechanism of residual stress

During wire sawing, most of the materials is sawn by fragile removal, and only a small part of the material is sawn by plastic removal. Fragile removal of materials mainly focus on the cutting area under wire saw, residual stress gradually disappears on the surface after some part of the materials fracture. However, plastic removal materials are mainly concentrated on both sides of the wire saw. When the materials are scratched by abrasives through plastic removal mode, the residual stress field will be generated under the abrasives and eventually affect the surface of the workpiece.

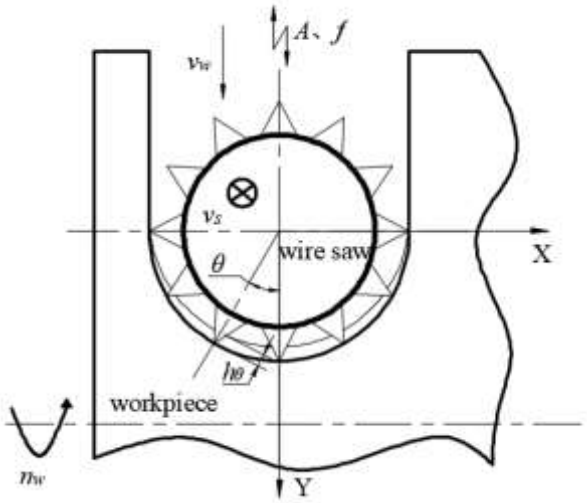

Fig. 2. Schematic diagram of wire sawing

Li et al. [25] proposed that the abrasives pressing depth h_θ at any wire saw cross section position is:

$$h_\theta = \sqrt{\frac{v_w cos\theta}{Ctanjv_s}} \tag{1}$$

Where, θ is the position angle of abrasives on the section of wire saw; C is the number of abrasive particles unit area; J is the half-cone angle of the abrasive.

Chen et al. [26] obtained the critical pressing depth h_c formula of material change from fragile deformation to plastic deformation under single grinding abrasive through both theoretical and experimental research：

$$h_c = 0.15K\left(\frac{E}{H_V}\right)\left(\frac{K_{IC}}{H_V}\right)^2 \tag{2}$$

Where, K is the correction parameter of external comprehensive influence, K<1; E is the elastic modulus; H_V is vickers hardness; K_{IC} is static fracture toughness.

When the pressing depth of abrasives is greater than the critical pressing depth, $h_\theta > h_c$, materials can be removed by brittle fracture, and it won't produce residual stress. When the pressing depth of abrasives is less than the critical pressing depth, $h_\theta < h_c$, the material removal method of abrasives is plastic removal, which will produce residual stress and eventually keep on the workpiece surface. When the pressing depth of abrasives is equal to the critical pressing depth, $h_\theta = h_c$, at this time, the abrasives are in the critical region, which is a kind of fragile plastic complexed removal method.

3. Finite element simulation of diamond wire sawing monocrystalline silicon

In the wire sawing process, material is mainly removed by brittleness, and plastic removal is supplemented. When the pressing depth of abrasives is less than the critical cutting depth, the material is removed in a plastic manner, resulting in residual stress, which will finally remain on the surface of the silicon wafer. In this paper, the model of diamond wire sawing monocrystalline silicon was established by ABAQUS, and the magnitude and distribution of residual stress on the silicon wafer surface after cutting were simulated and calculated.

3.1 Establish of simulation model

The temperature change is very small during the cutting process, then the effect of temperature on the residual stress is not considered, only the effect of the cutting action on the residual stress is considered. Fig. 3 shows the simulation model of wire sawing monocrystalline silicon. Since the Mohs hardness value of diamond abrasives is ten and that of monocrystalline silicon is six, and the bending condition during wire sawing is ignored, so the diamond wire saw is set as a rigid body without deformation. In order to improve the calculation accuracy and shorten the calculation time, the monocrystalline silicon workpiece was divided into two parts. The wire sawing area grid was refined, while the other area grid was slightly thicker.

In order to make the simulation more realistic and convincing, the cutting process adopts the D-P plastic constitutive model proposed by Drucker and Prager for geotechnical materials [27]. In the cutting process, when the shear stress on the main plane can overcome the viscous and sliding friction resistance, inelastic deformation occurs, and the yield condition is shown in Eq. (3):

$$f = \sqrt{3J_2} + \frac{1}{3} I_1 \alpha - k \tag{3}$$

Where: J_2 is the second invariant of the deviatoric stress tensor S, I_1 is the first invariant of the stress tensor, α is the pressure sensitivity coefficient, and k is the cohesion of the material.

In the cutting process, the separation criterion adopts the shear failure criterion. According to whether the equivalent plastic strain at the element integration point reaches the set value, it is determined whether the element fails.

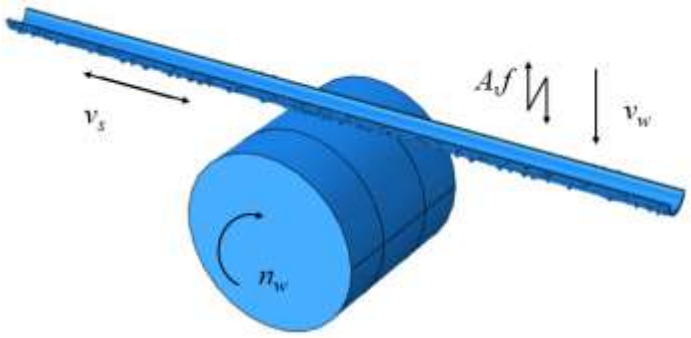

Fig. 3. Simulation model of diamond wire sawing monocrystalline silicon

After constraint is imposed and mesh is divided, process parameters are set in the software. Table 1 shows simulational parameters of diamond wire sawing.

Table 1 Diamond wire sawing simulation parameters

Parameters	Value
The axial speed (m/s)	2,4,6,8
Feed speed (mm/min)	1,2,3,4
Rotation speed (r/min)	10,20,30,40
Ultrasonic frequency (Hz)	20000
Ultrasonic amplitude (μm)	10

3.2 Analysis of the simulation results about residual stress

Fig. 4 shows the simulation process of diamond wire sawing monocrystalline silicon. Fig. 4 (a) shows the contact stage between the wire saw and the workpiece. When the abrasive particles on the wire saw contact the workpiece, the stress value in the machining area increases instantly, but

does not reach the yield strength of the workpiece. Fig. 4 (b) and Fig. 4 (c) show the fracture removal stage of the material. The material in the processing area starts to break after reaching the yield strength so that the material is removed. Fig. 4 (d) shows the finish stage of machining, in which the cylindrical workpiece is cut into two sections.

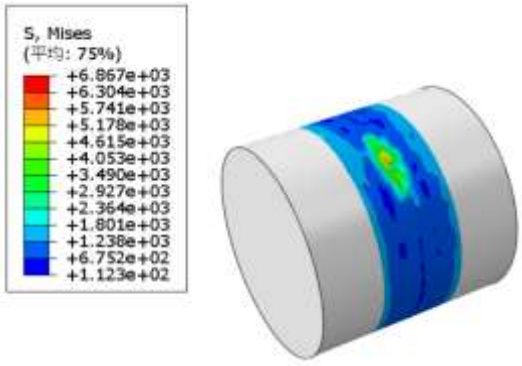

(a) The contact stage

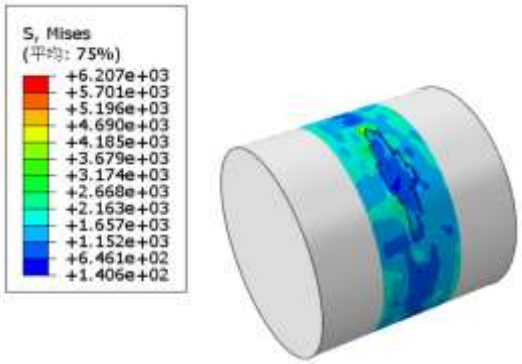

(b) Fracture stage of material

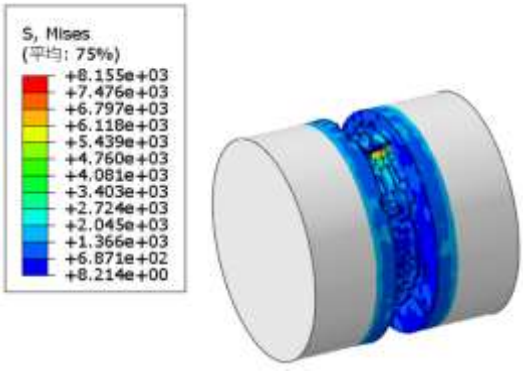

(c) Material removal stage

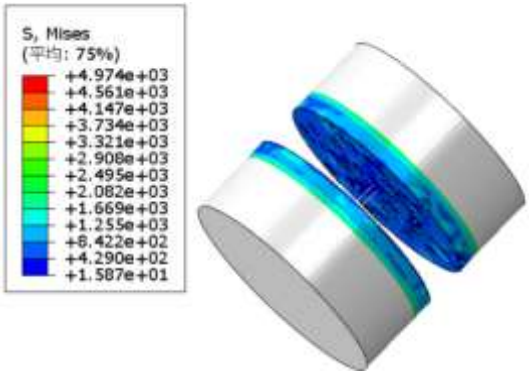

(d) The cutting finish stage

Fig. 4. Simulation process of diamond wire sawing monocrystalline silicon

The machined surface of conventional wire sawing and ultrasonic vibration assisted wire sawing are shown in Fig.5. The number of pits on the machined surface of the workpiece after ultrasonic vibration assisted is less and the surface quality is better. The abrasive particles on the side of the wire saw scrape and polish the machined surface, so that the stress keeps on the surface of the silicon wafer.

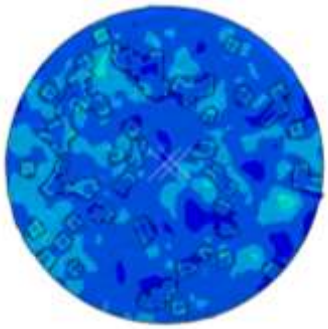

(a) Machined surface by conventional wire sawing

(b) Machined surface by ultrasonic vibration assisted wire sawing

Fig. 5. Comparison of surface by conventional and ultrasonic vibration assisted wire sawing

The extraction of residual stress requires unloading the workpiece after the wire sawing is completed, removing all the displacement constraints and interactions during machining, and averaging the values of the ten points on the surface.

(1) Effect of axial line speed of wire saw on surface residual stress

It can be seen from the Fig.6, monocrystalline silicon wafer surface keeps compressive stress whether or not ultrasonic vibration assistance. When both the workpiece rotation speed and the wire saw feed speed are constant, the residual compressive stress on the wafer surface increases with the axial speed of the wire saw from 2m/s to 8m/s. The residual compressive stress on silicon wafer surface in ultrasonic vibration assisted wire sawing is larger than that in conventional wire sawing.

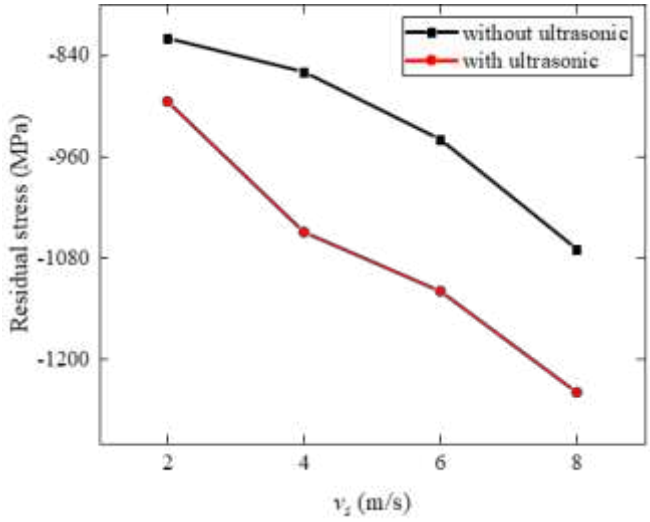

Fig. 6. Effect of axial speed of wire saw on residual stress

(2) Effect of feed speed on surface residual stress

It can be seen from Fig. 7 that the surface of monocrystalline silicon keeps compressive stress regardless of whether or not ultrasonic vibration is applied. When the workpiece rotation speed and the axial speed of the wire saw are constant, the residual compressive stress on the surface of the silicon wafer decreases with feed speed from 1mm/min to 4mm/min, and the residual compressive stress on the surface of the silicon wafer in ultrasonic vibration assisted wire sawing is larger than that in conventional wire sawing.

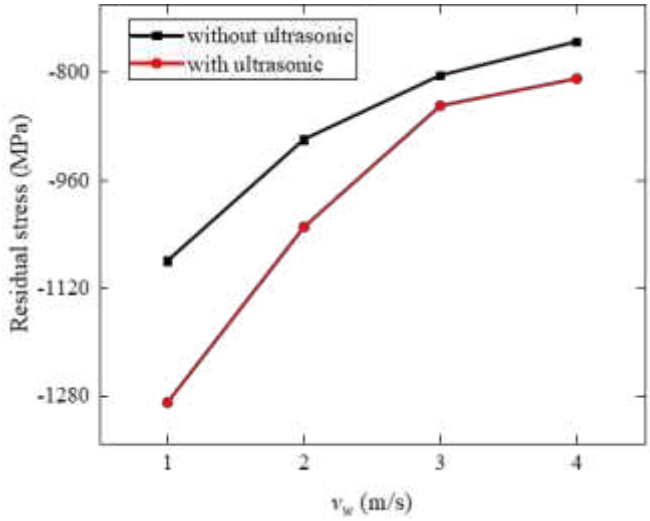

Fig. 7. Effect of the feed speed on residual stress

(3) Effect of workpiece rotation speed on surface residual stress

It can be seen from Fig. 8 that the surface of monocrystalline silicon is under compressive stress regardless of whether ultrasonic vibration is applied. When the feed speed and axial speed of the wire saw are constant, the residual compressive stress on the surface of the silicon wafer does not change much with the workpiece rotation speed from 10 r/min to 40 r/min. The residual compressive stress on the surface of the silicon wafer in ultrasonic vibration assisted wire sawing is larger than that in conventional wire sawing.

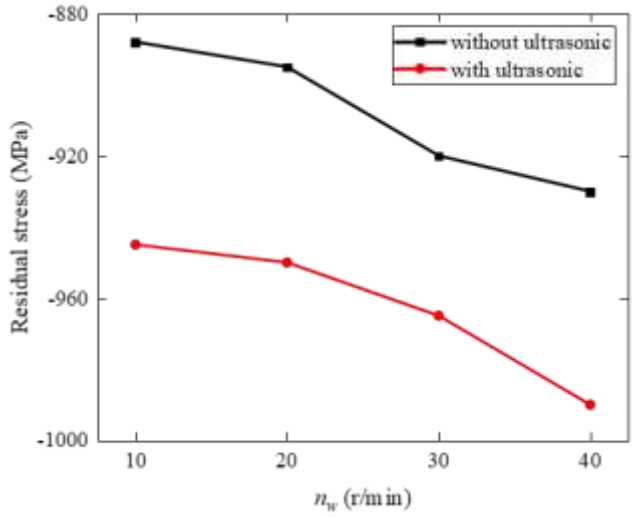

Fig. 8. Effect of workpiece rotation speed on residual stress

4. The experiment of ultrasonic vibration assisted diamond wire sawing

In order to verify the correctness of the above theoretical model, a reciprocating diamond wire saw slicing machine CHSX5630-XW was used to conduct ultrasonic vibration-assisted diamond wire saw experiment, and the residual stress on the silicon wafer was detected by blind hole method.

4.1 Experimental setup

The experimental and the detection equipment are shown in Fig. 9. Monocrystalline silicon workpiece is cylindrical body with diameter of 35mm and length of 50mm. The saw wire is electroplated with 0.45mm diameter diamond abrasives. The total length of saw wire is 150m, and the average diameter of diamond abrasives is 50μm. During the slicing process, the tensioning force of the diamond wire saw machine is constant. The ultrasonic generator is a self-built test platform. The ultrasonic amplitude of the ultrasonic generator is 10μm and the frequency is 20KHz. DWS vibration displacement sensor is used to monitor the vibration of wire saw in real time.

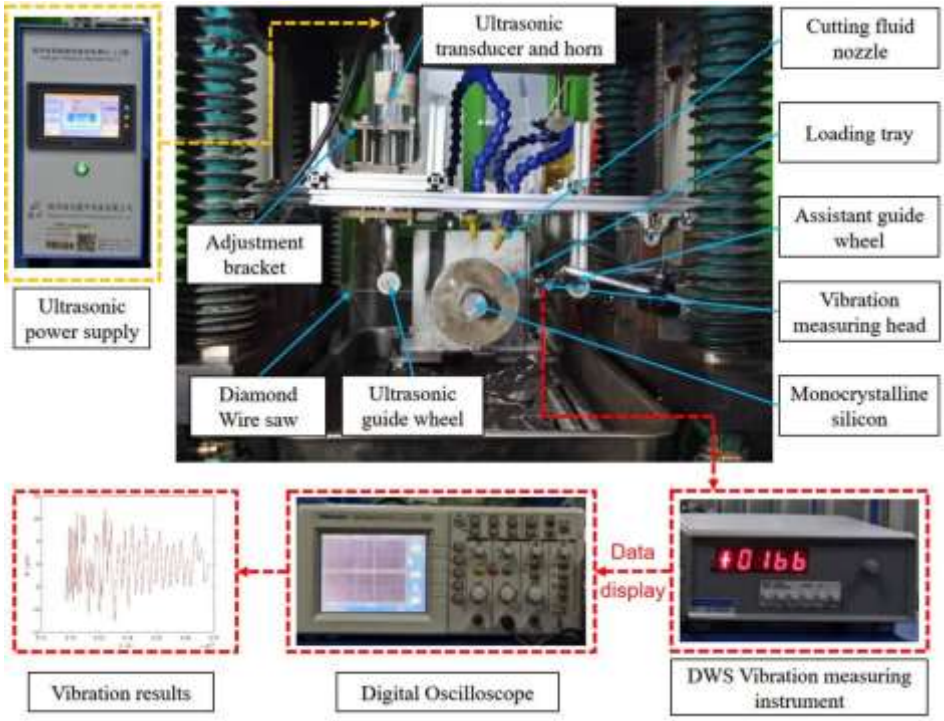

Fig. 9. Ultrasonic vibration assisted wire sawing monocrystalline silicon experimental and detection equipment

In this experiment, the three factors that have the greatest influence on residual stress were selected to carry out the three-factor and three-level experiment. The factors are as follows: the axial speed of wire saw v_s (m/s), wire saw feed speed v_w (mm/min), workpiece rotation speed n_w (r/min). Three levels were selected for each factor, covering common range of slicing parameters, and the level values were evenly distributed within the selected range. Orthogonal experiments parameters were shown in Table 2. For each group of slicing parameters, conventional wire sawing and ultrasonic vibration assisted wire sawing were performed.

Table 2 Orthogonal experiment parameters

Group	v_s(m/s)	v_w(mm/min)	n_w(r/min)
1	2	1	10
2	2	2	30
3	2	3	50
4	5	1	30
5	5	2	50
6	5	3	10
7	8	1	50
8	8	2	10
9	8	3	30

4.2 Principle of measuring residual stress by blind hole drilling method

Fig. 10 shows the blind hole drilling method of measuring residual stress diagram. Blind hole method measures residual stress based on the mechanism of stress release. The workpiece surface pasted with certain shape and size of the strain gauges to form three-way strains of flower, then at the geometric center of three-way strain rosette according to certain diameter drilling, breaking the

stress balance inside the workpiece, the stress redistribution inside the workpiece reaches the quadratic balance. The strain values ε_1、ε_2 and ε_3 before and after drilling were measured by a strain gauge of a certain specification. According to the theory of elasticity, the principal stresses σ_1 and σ_2 and the principal direction angle φ of this point can be calculated by the relationship between stress and strain.

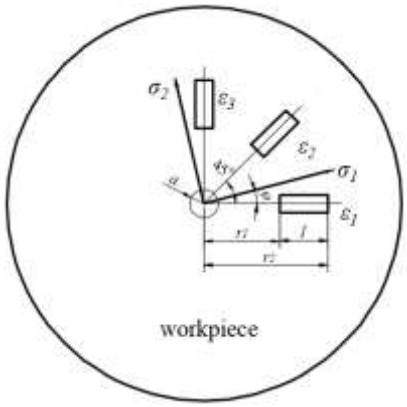

Fig. 10. Schematic diagram of principle of measuring residual stress by blind hole drilling method

Li et al. [28] gave the relationship between principal stress, principal direction angle and strain in the blind hole drilling method.

$$\sigma_{1,2} = \frac{1}{4A}(\varepsilon_1 + \varepsilon_2) \pm \frac{\sqrt{2}}{4B}\sqrt{(\varepsilon_1 - \varepsilon_2)^2 + (\varepsilon_3 - \varepsilon_2)^2} \tag{4}$$

$$tan2\varphi = \frac{\varepsilon_1 + \varepsilon_3 - 2\varepsilon_2}{\varepsilon_1 - \varepsilon_3} \tag{5}$$

Where, φ is the included angle between 0° strain gauge and the direction of the first principal stress of residual stress σ_1; ε_1、ε_2 and ε_3 are the strain in three directions, and σ_1 and σ_2 are the principal stresses in two directions.

In the through-hole state, the theoretical solutions of release coefficients A and B are shown in Eqs. (6) and (7):

$$A = -\frac{a^2(1+\mu)}{2Er_1r_2} \tag{6}$$

$$B = \frac{2a^2}{Er_1r_2}\left[\frac{(1+\mu)a^2(r_1^2 + r_1r_2 + r_2^2)}{4r_1^2r_2^2} - 1\right] \tag{7}$$

Where, μ is the Poisson's ratio; a is the diameter of the hole; r_1 and r_2 are the distances from the center of the hole to the proximal and distal ends of the strain gauge, respectively.

In this paper, the blind hole drilling method is used to measure the residual stress, and there is a certain degree of difference between the release coefficient and the through hole method. Lin et al. [29] gave the relationship between the release coefficient in the blind hole state and the through hole state. The strain release coefficient A when drilling blind holes is not much different from that when drilling through holes, so the above formula can be used to calculate the value when drilling blind holes, but there is a coefficient difference, usually 1.065. The difference between the strain release coefficient B when drilling blind holes is very small compared with that when drilling through holes, so Eqs. (7) can be used to directly calculate the value of strain release coefficient B when drilling blind holes.

Fig. 11 is the experimental platform for measuring residual stress by blind hole drilling method.

Although the residual stress measured by blind hole method is a lossy detection, its damage degree to the workpiece is very small.

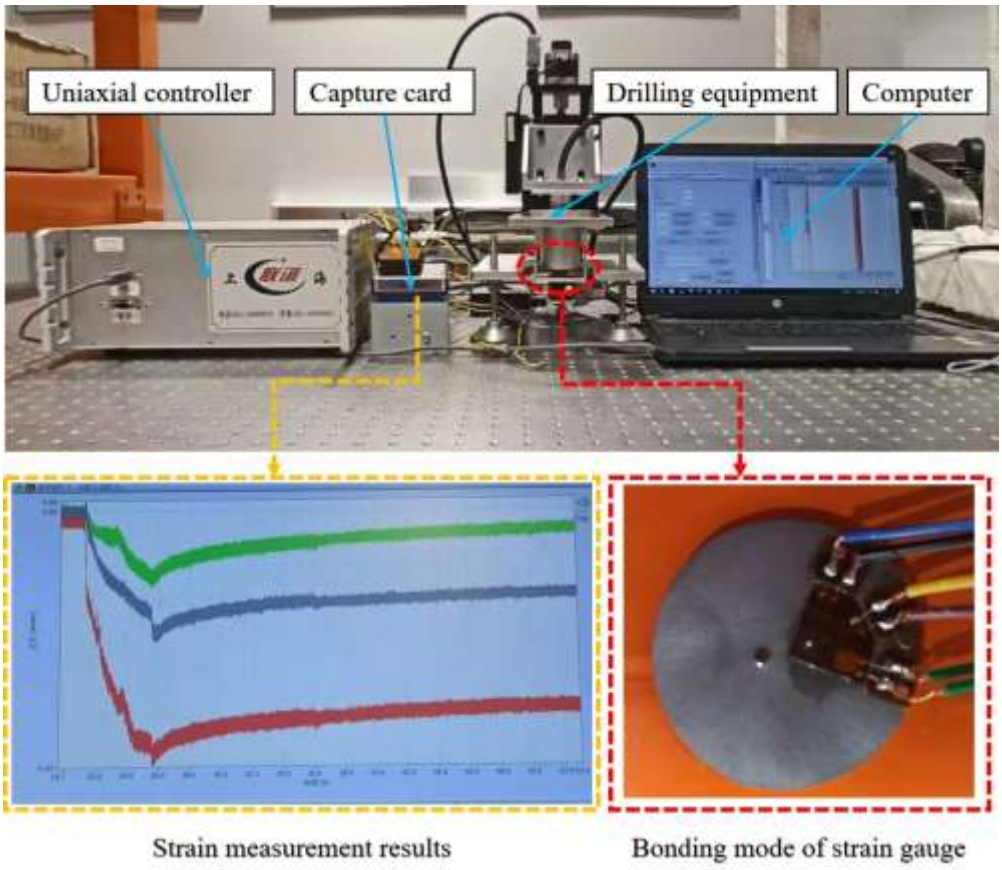

Fig. 11. Experiment platform for measuring residual stress by blind hole drilling method

Because the surface quality of the workpiece after wire sawing is good, there is no need to polish the workpiece surface, and the strain gauge is directly bonded on the surface of the silicon wafer. A BF350-3CA strain gauge with resistance R = 350 Ω is used in the experiment. After the strain gauge being pasted on the surface of the workpiece, the lead wire and the lead wire are welded together through the internal heat soldering iron. The strain gauge was connected with the strain acquisition instrument by a 1/4 bridge connection, and the drilling instrument was used to drill the blind hole with diameter 1mm and depth 0.1mm. After drilling, the corresponding values could been read after the strain was stabilized.

5. Experimental results and analysis

The strain values before and after drilling can be measured by blind hole drilling method under different slicing parameters, and the residual stress of the monocrystalline silicon wafer can be obtained by combining with theoretical calculation. During wire sawing, three pieces of silicon wafers are cut under the same processing parameters, and the strain gauge is used to measure at the same position of each piece of silicon wafer. The residual stress value of each group is calculated by theoretical formula, and the average value is taken as the residual stress on the surface of the silicon wafer. Table 3 shows the residual stress on the surface of the silicon wafer after the conventional wire sawing. Table 4 shows the residual stress on the surface of the silicon wafer after the ultrasonic vibration assisted wire sawing. It can be obtained that the residual stress on the surface of the silicon wafer after the diamond wire sawing is the compressive stress.

Table 3 The residual stress on the surface of the silicon wafer in conventional wire sawing

Group	v_s(m/s)	v_w(mm/min)	n_w(r/min)	σ_1(MPa)	σ_2(MPa)
1	2	1	10	-73.78	-92.55
2	2	2	30	-54.04	-55.55
3	2	3	50	-15.00	-26.18
4	5	1	30	-94.92	-104.89
5	5	2	50	-104.18	-126.14
6	5	3	10	-19.33	-23.44
7	8	1	50	-117.57	-168.73
8	8	2	10	-71.73	-129.55
9	8	3	30	-124.55	-81.72

Table 4 The residual stress on the surface of the silicon wafer in ultrasonic vibration assisted wire sawing

Group	v_s(m/s)	v_w(mm/min)	n_w(r/min)	σ_1(MPa)	σ_2(MPa)
1	2	1	10	-96.18	-150.17
2	2	2	30	-75.02	-130.23
3	2	3	50	-23.49	-72.54
4	5	1	30	-129.93	-179.57
5	5	2	50	-112.25	-141.78
6	5	3	10	-116.48	-139.48
7	8	1	50	-167.76	-179.48
8	8	2	10	-121.67	-156.22
9	8	3	30	-81.50	-145.17

5.1 Analysis of residual stress

(1) Effect of the axial speed of wire saw on surface residual stress

Fig. 12 shows the variation trend of residual stress with the axial speed of wire saw, it can be seen that the residual compressive stress on the surface of the wafer increases with the increase of the axial speed of wire saw v_s from 2m/s to 8m/s. With the increase of the axial speed of wire saw, the larger contact area between the abrasives on the saw and the workpiece per unit time, thus the average pressing depth of the abrasives decreases, making more abrasives on the side of the saw removed in a plastic mode, resulting in the increase of residual compressive stress on the surface of the silicon wafer.

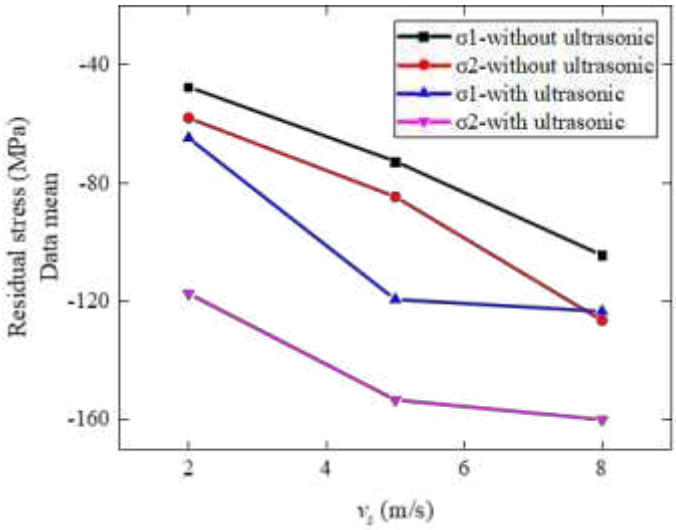

Fig. 12. Effect of the axial speed of wire saw v_s on residual stress

(2) Effect of wire saw feed speed on surface residual stress

Fig. 13 shows the variation trend of residual stress with the wire saw feed speed, it can be seen that the residual compressive stress on the surface of the silicon wafer decreases as the wire saw feed speed increases from 1mm/min to 3mm/min. The reason is that with the continuous increase of feed speed, more materials need to be removed per unit time. The grinding pressing depth on the side of the wire saw exceeds the critical pressing depth and the workpiece materials is removed in a fragile removal mode, resulting in a smaller residual pressure stress on the surface of the silicon wafer.

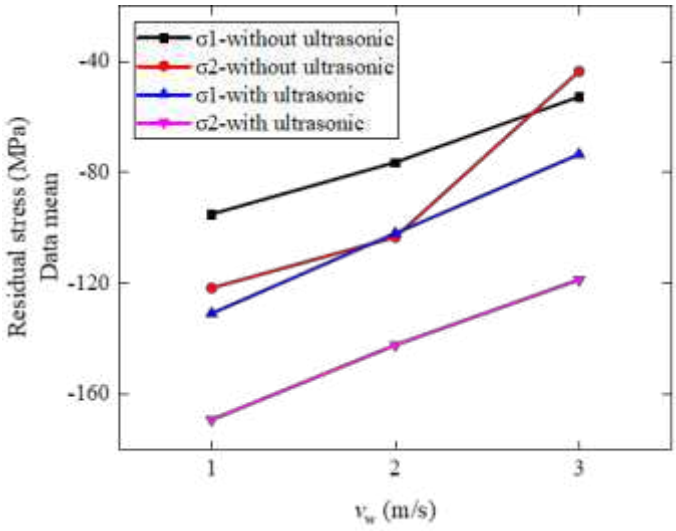

Fig. 13. Effect of wire saw feed speed v_w on residual stress

(3) Effect of workpiece rotation speed on surface residual stress

Fig. 14 shows the variation trend of residual stress with the workpiece rotation speed, it can be seen that the residual compressive stress on the surface of the silicon wafer fluctuates with the increase of workpiece rotation speed n_w from 10 r/min to 50 r/min. On the one hand, the workpiece rotation speed can be equivalent to a part of the axial speed of wire saw, but the speed has little influence on the axial speed of wire saw. On the other hand, the workpiece rotation makes the wire saw better for the secondary processing of the machined surface, but the removal amount is very small, and the influence on the residual compressive stress is also very small.

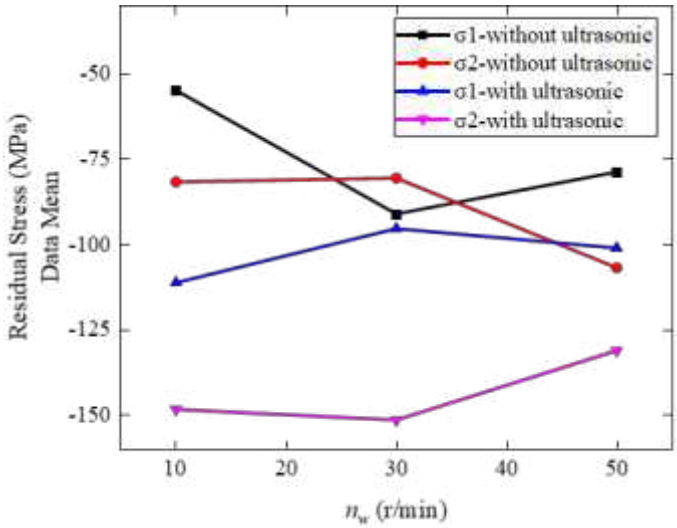

Fig. 14. Effect of workpiece rotation speed n_w on residual stress

(4) Effect of ultrasonic vibration on surface residual stress

It can be seen from Fig. 12, Fig. 13 and Fig. 14, the residual compressive stress under ultrasonic vibration assisted wire sawing monocrystalline silicon is larger than that of conventional wire sawing while the axial speed of wire saw v_s ,wire saw feed speed v_w and workpiece rotation speed n_w are fixed. The reasons can be analyzed as follows: Diamond wire saw cuts monocrystalline mainly in a fragile removal mode, and the flanked areas are removed in a plastic removal mode. With ultrasonic vibration assisted, the abrasives with high frequency vibration and smash properties can effectively reduce the average sawing force in machining and increase the critical pressing depth [30]. The pressing depth of more abrasives on the side of wire saw is less than the critical pressing depth and removed in a plastic mode, resulting in an increase of residual pressure stress on the surface of the silicon wafer.

5.2 Analysis of surface topography

After the wire sawing was completed, the surface of the silicon wafer was detected with the KEYENCE VHX-6000 optical microscope. The surface topography of silicon wafer by conventional wire sawing and ultrasonic vibration assisted wire sawing is shown in Fig. 15.

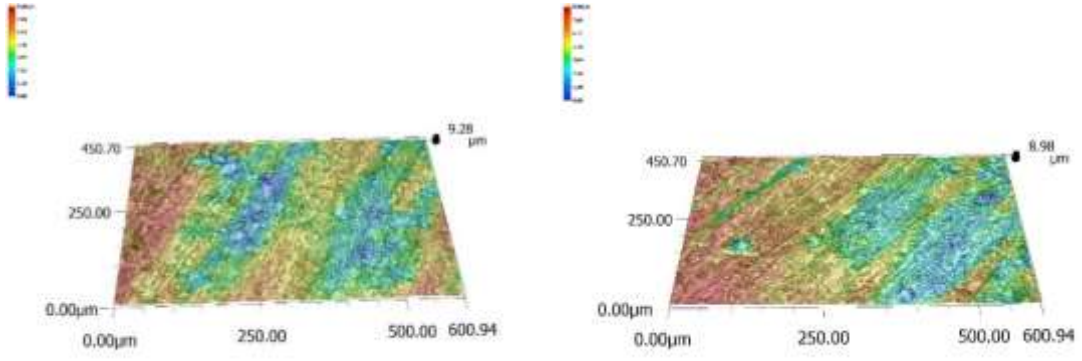

(a) Surface topography of silicon wafer by conventional wire sawing

(b) Surface topography of silicon wafer by ultrasonic vibration assisted wire sawing

Fig. 15. Comparison diagram of silicon wafer surface morphology

It can be seen from Fig. 15, under the same process parameters, there are many large pits on the surface of the workpiece by conventional wire sawing. The surface of the workpiece by ultrasonic vibration assisted wire sawing is relatively smooth, and the reason for the small size of

pits is that the abrasive particles impact the workpiece in a short time under ultrasonic vibration excitation. In the ultrasonic vibration cycle, the impact of abrasive particles on the workpiece cutting times are more but the contact time is very short, so the workpiece is easy to be broken into micron and submicron fragments, the size of pits also becomes smaller. Secondly, the ultrasonic vibration changes the trajectory of the abrasive particles, and the abrasive particles rub the workpiece surface repeatedly, which is beneficial to remove the peak of the residual scratches and improve the surface quality of the workpiece.

6. Conclusion

In this paper, the surface residual stress of ultrasonic vibration assisted diamond wire sawing monocrystalline silicon wafer was measured based on the blind hole drilling method. The distribution of residual stress under different process parameters was obtained through wire sawing simulation, and the following conclusions were drawn:

(1) By measuring the strain value of the silicon wafer before and after drilling with the blind hole drilling method, the principal stresses in two directions are calculated according to the theoretical formula of stress-strain, and it is concluded that the residual stress on the surface of the diamond wire sawing monocrystalline silicon is mainly compressive stress.

(2) The simulation model of diamond wire sawing monocrystalline silicon was established by ABAQUS based on D-P constitutive, and the variation trend of residual stress under different process parameters was obtained, which was verified by experiments. The results showed that the residual compressive stress on the wafer surface increases with the increase of the axial speed of wire saw and wire saw feed speed. The residual compressive stress on the wafer surface decreases gradually with the increase of the workpiece rotation speed, the residual compressive stress on the surface of the wafer doesn't show any significant change. Under the same process parameters, the residual compressive stress on the surface of silicon wafer by ultrasonic vibration assisted diamond wire sawing is larger than that of conventional wire sawing, and a certain degree of residual compressive stress can improve the anti-fatigue property of silicon wafer.

(3) By observing the surface morphology of silicon wafer after sawing, it can be seen that under the same process parameters, the surface morphology of silicon wafer cut by ultrasonic vibration assisted wire sawing is better than that by conventional wire sawing. The number of pits on silicon wafer cut by ultrasonic vibration assisted wire sawing is less, the size of pits is smaller, and the surface quality is improved.

Acknowledgement

The authors thank the Natural Science Foundation of Shanghai for supporting for the study.

Authors' Contributions: Yan Wang: Conceptualization, Methodology, Supervision, Writing-Review & Editing. Bocheng Zhao: Formal analysis, Writing-Original Draft. Jixing Li: Visualization, Software. Zhaofeng Qian: Investigation, Data curation. Shengju Huang: Investigation. Jinhuan Su: Resources. Jing Zhou: Resources.

Funding: No funding was received for conducting this study.

Data availability: The manuscript has no associated data or the data will not be deposited.

Declarations

Conflict of interest: The authors declare that they have no competing interests.

Ethical approval: This work has not been published elsewhere.

Code availability: Not applicable.

Consent to Participate: Not applicable.

Consent for publication: Not applicable.

References

[1] Jiao F, Niu Y, Zhao B (2017) Research Progress of Residual Stress in Milling of Difficult-to-machine Materials. Surf Sci 46(3):267-273

[2] Wu Z, Zhou J, Chen W (2015) Effects of residual stress on the electrical properties in PbZr0.52Ti0.48O3 thin films. J Solgel Sci Technol 75(3):551-556

[3] Lee JW, Park GT, Park CS (2006) Enhanced ferroelectric properties of Pb (Zr,Ti) O-3 films by inducing permanent compressive stress. Appl Phys Lett 88:72908

[4] Ma XM, Ou QY (2019) Study for inverse hole-drilling method applied on residual stress measurement of inner surface. China Measurement & Test 45(5):26-32+37

[5] Zheng TY, Danyluk S (2001) Nondestructive Measurement of in Plane Residual Stresses in Thin Silicon Substrates by Infrared Transmission. Materials Evaluation 59:1227-1233

[6] Popovich VA, Westra JM, Van SR (2011) Raman spectroscopy characterization of residual stress in multicrystalline silicon solar wafers and solar cells; relation to microstructure, defects, and processing conditions. 37th IEEE Photovoltaic Specialists Conference

[7] Babaeeian M, Mohammadimehr M (2021) Experimental and computational analyses on residual stress of composite plate using DIC and Hole-drilling methods based on Mohr's circle and considering the time effect. Opt Lasers Eng 137:106355-

[8] Zhou P, Wang ZG, Yan Y, Huang N, Kang RK, Guo DM (2020) Sensitivity analysis of the surface integrity of monocrystalline silicon to grinding speed with same grain depth-of-cut. Adv Manuf 8(1):97-106

[9] Jiao SS, Huang QM, Tu WJ, Chen J, Sun ZM (2019) Investigation on the phase transformation of monocrystalline silicon during nanoindentation at cryogenic temperature by molecular dynamics simulation. Physica B Condens Matter 555(1):139-144

[10] Echizenya D, Sakamoto H, Sasaki K (2011) Effect of mechanical surface damage on silicon wafer strength. Proc Eng 10(C):1440-1445

[11] Wurzner S, Buchwald R, Retsch S (2015) Investigation of the development of the microcrack structure in scratch tests with single diamond particles on monocrystalline silicon wafers. 29th European Photovoltaic Solar Energy Conference and Exhibition 742:-6

[12] Dai HF, Chen GY, Zhou C, Fang QH, Fei XJ (2017) A numerical study of ultraprecision machining of monocrystalline silicon with laser nano-structured diamond tools by atomistic simulation. Appl Surf Sci 393(1):405-416

[13] Yang C, Mess F, Skenes K (2013) On the residual stress and fracture strength of crystalline silicon wafers. Appl Phys Lett 102

[14] Kumar A, Prasath RG, Pogue V (2016) Effect of Growth Rate and Wafering on Residual Stress of Diamond Wire Sawn Silicon Wafers. Procedia Manuf 5:1382-1393

[15] Costa EC, Santos CP, Xavier FA (2020) Experimental Investigation of the Sawn Surface of Monocrystalline Silicon Cut by Endless Diamond Wire Sawing. Mater Res 23(4)
[16] Yang M, Peng F, Yan R, Deng B, Zhou L, Wang H (2019) Study on the surface damage mechanism of monocrystalline silicon in micro ball-end milling. Precis Eng 56(0):223-234
[17] Pogue V, Melkote SN, Danyluk S (2018) Residual stresses in multi-crystalline silicon photovoltaic wafers due to casting and wire sawing. Mater Sci Semicond Process 75:173-182
[18] Banerjee S, Yang JT, Wu JN (2017) Phase and stress evolution of Si swarf in the diamond-coated wire sawing of Si ingots. Int J Adv Manuf Technol 89(1-4):735-742
[19] Kiyota H, Hara K, Jankowski M (2020) Numerical simulation and validation of subsurface modification and crack formation induced by nanosecond-pulsed laser processing in monocrystalline silicon. J Appl Phys 127(8):1-11
[20] Zhang XH, Luo MM, Xu XX, Zhao B (2016) Numerical Simulation on Residual Stress of Titanium Alloy Surface Aided with Ultrasonic Vibration Cutting. Computer Simulation 33(5):208-211
[21] Chen P, Zhang ZW, An T, Yu HP, Qin F (2018) Generation and distribution of residual stress during nano-grinding of monocrystalline silicon. Jpn J Appl Phys 57(12):121302
[22] Liu HJ, Han J, Tian XQ, Dong FF, Chen S, Lu L (2019) Accurate determination of bifurcation points for ground silicon wafers considering anisotropy using FEM method. Mater Res Express 6(9):095906
[23] Liu HJ, Zhou J, Han J, Tian XQ, Chen S, Lu L (2021) Evaluation of polishing-induced subsurface damage based on residual stress distribution via measured global surface deformation for thinned silicon wafers. Surface Topography: Surf Topogr 9(3):035001
[24] Xu DH, Guo Q, Zhang HB, Zhang MY (2019) Finite element simulation of surface residual stress in ultrasonic vibration cutting of aluminum alloy. Journal of Mechanical＆Electrical Engineering 36(12):1242-1247
[25] Li SJ, Liu Y, Hou XL, Gao XQ (2015) Analysis and Modeling Cutting Force for SiC Monocrystal Wafer Processing. J Eng Mech 51(23):189-195+204
[26] Chen MJ, Zhang FH, Dong S, Li D (2001) Study on Ultra-Precision Grinding of Optical Glasses in the Ductile Mode. Chin J Mech Eng-En (04):101-103+125+8-9
[27] Drucker DC, Prager W (1952) Soil mechanics and plastic analysis for limit design. Q Appl Math 10(2):157-165
[28] Li W, Yu L, Wang X (2013) Test of residual stress by hole drilling strain method. Electrical Steel 51(6):55-59
[29] Li Q (2014) Research on the Influence of Hardened Steel 40CrNiMo Residual Stress by Turning Parameters. Zhengzhou University
[30] Li L, Li SJ, Tang AF, Li Y (2016) Influence of Diamond Wiresaw Excited by Transverse Ultrasonic Vibration on Cutting Force and Critical Cutting Depth of Hard and Brittle Materials. J Eng Mech 52(3):187-196